Soares Oliveira, Rafael; Machado, Renato R.; Lepikson, Herman; Fröhlich, Thomas; Theska, René:

A method for the evaluation of the response of torque transducers to dynamic load profiles

Original published in:	Acta IMEKO / International Measurement Confederation. - Braunschweig. - 8 (2019), 1, p. 13-18.
Original published:	2019-08-02
ISSN:	2221-870X
DOI:	10.21014/acta_imeko.v8i1.654
[*Visited:*	2019-07-09]

ACTA IMEKO
ISSN: 2221-870X
March 2019, Volume 8, Number 1, 13 - 18

A method for the evaluation of the response of torque transducers to dynamic load profiles

Rafael S. Oliveira[1], Renato R. Machado[1], H. Lepikson[2], Thomas Fröhlich[3], René Theska[3]

[1] *Instituto Nacional de Metrologia, Qualidade e Tecnologia - INMETRO, Duque de Caxias, Brazil*
[2] *Federação das Indústrias do Estado da Bahia - FIEB, Salvador, Brazil*
[3] *Technische Universität Ilmenau - TU-ILMENAU, Ilmenau-TH, Germany*

ABSTRACT
The traceability of the torque quantity finds a gap when there is a regime with torque variation rates. The traditional calibration methods define the references to be on the static regime, with null torque rates. This paper presents a method for providing torque traceability to rotating sensors under high torque variation rates. The principle of applying acceleration pulses to rotating shafts, with mounted reference discs with known mass moments of inertia thereon, is presented herein, followed by a description of sequential proceedings for obtaining an analysis in the time domain. The development of the uncertainty budget is also discussed. Demonstrative experimental data is used in order to ratify the principle and to maintain a qualitative approach to the theoretical description of these methods. The research gives a very good idea of the necessary different future approaches to guarantee traceability for mechanical quantities.

Section: RESEARCH PAPER

Keywords: Dynamic torque; torque metrology; high torque variation rate; torque transducer; angular acceleration

Citation: Rafael S. Oliveira, Renato R. Machado, Herman Lepikson, Thomas Fröhlich, René Theska, A method for the dynamic calibration of torque transducers using angular speed steps, Acta IMEKO, vol. 8, no. 1, article 3, March 2019, identifier: IMEKO-ACTA-08 (2019)-01-03

Editor: Petri Koponen, MIKES Metrology, Finland

Received August 3, 2018; **In final form** November 16, 2018; **Published** March 2019

Corresponding author: Rafael S. Oliveira, e-mail: rsoliveira@inmetro.gov.br

1. INTRODUCTION

The current traceability methods for torque transducers used in all applications are based on static proceedings and static standard systems. Traditional calibration standards and guidelines, such as [1], define the reference value as a completely static one, preferably using a dead weight and lever-arm torque generation machine, accompanied by a large period of stabilization during the load sequences.

However, in regimes in which it is important to measure torque during periods with high torque rates, there must be a demand for different patterns. In addition, most of these applications also use sensors under rotation conditions, which is also not considered in the traditional standard to a great degree. Traceability alternatives must be found in order to cover these non-static measurement systems.

The research on new methods of providing traceability to the torque quantity is growing [2]-[4], and the dynamic approach is also becoming a key area of the research. This paper makes significant contributions to this research field, and this proposal, first introduced in [5]-[8] and now reviewed in detail, fits into the dynamic metrology scenario. There are different interpretations of the definitions or statements concerning how dynamic can measurements be.

1.1. The Dynamics of the Proposal

To understand the dynamic basis of the proposal, it is important to point out two main facts that delineate the extremes into which it fits.

First approaches to the traceability of dynamic torque were presented in [9]-[9], where an oscillatory (sinusoidal) regime was applied to the measurement system through a frequency range sweep, followed by the frequency domain analysis of the data. This method evaluates both the amplitude and phase responses of the device under calibration.

On the other hand, [1] presents the continuous calibration method as an alternative to the static one, which can reduce the total calibration time in 1/10. However, beyond the necessity of the equipment being able to detect fast readings, instead of stabilised ones, rapid changes in torque values cause unwanted effects on transducer behaviour, such as creep phenomena and high reversibility errors [11]. A critical torque rate of around 17 $N \cdot m \cdot s^{-1}$ during incremental loading is found in [12], where the linearity deviation results are very disturbed. In [13], it is shown

that the different digital filtering parameters and the rates of torque application directly influence the stability of the readings. These behaviours can be attributed to dynamic effects and cannot therefore be followed by a simple continuous quasi-static loading methodology.

Therefore, within these two extremes, one question remains: How can traceability be covered for loading torque profiles, with high rates of variation of quantity and keeping direct analysis to the time domain?

The research presented in this paper keeps the analysis in the time domain, being interpreted and summarised as a next step in the generation of reference torque pulses (no oscillations) with high torque rates, together with the sensor's rotation regimes, when the continuous torque calibration proceeding becomes insufficient.

2. CALIBRATION METHOD AND DESCRIPTION

As already introduced in [2], the proposed method is based on the principle of applying reference dynamic torque (T) to the transducer through the acceleration ($\dot{\omega}$) of a part with a known mass moment of inertia, MMI (θ), as calculated in equation (1).

$$T = \theta \cdot \dot{\omega} \tag{1}$$

In a rotating shaft, the proposed dynamic regime corresponds to the acceleration pulse period between two angular speed steps. With the speed signal measured, acceleration data can be obtained through its differentiation.

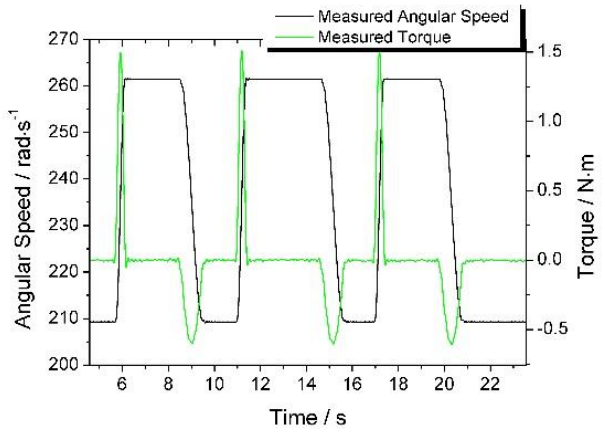

Figure 1. Angular speed steps and measured torque pulses.

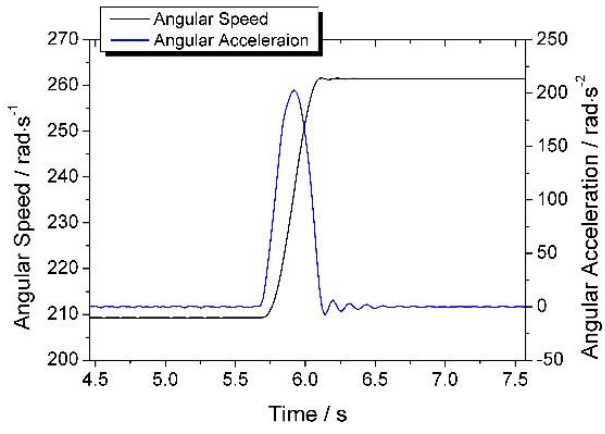

Figure 2. Angular speed step with calculated angular acceleration pulse.

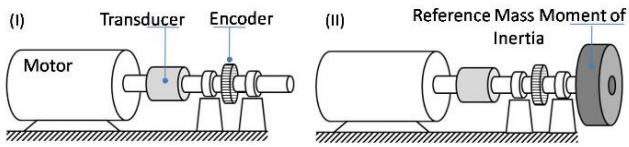

Figure 3. Assembly with the sensor in line with different configurations of inertia.

It is important to highlight that the start-ups are done with the whole system under rotation. Therefore, there are ramps between speed steps, where the reference acceleration is extracted, and the speed is then returned for the previous step through a braking period. Figure 1 shows an example of this regime in time, with a system comprising an electric motor, an encoder, and a torque transducer coupled with it (see configuration I in Figure 3), running three consecutive acceleration ramps between speed steps.

Figure 2 shows a zoom-in view of the time axis, with the measured speed signal and the calculated acceleration pulse during the speed step period. This period of acceleration pulse corresponds to the possibility of applying high torque rates, and the development of strategies for reaching the torque traceability during this regime is the challenge considered in this research.

Broadly, the proposed method should:

- Identify the time dependency of the quantity;
- Prioritise the application of torque rates;
- Evaluate the differences between the values read in the transducer (calibration curves) and those generated in the reference;
- Evaluate susceptibility to different kinematic conditions;
- Occur throughout the range of application of torque; and
- Assess reproducibility in sequential loadings.

2.1. SEQUENCE OF OPERATION

A sequence of operation is proposed in order to get a logical path to reach the intended torque profiles to better evaluate the sensor under different kinematic conditions. Figure 3 shows the proposed mechanical system, including the driver (electric motor), the transducer, the encoder, and the inertial shaft.

Configuration I shows the initial assembly with the main, the constants, and the components of inertia in the shaft, which will be called the initial mass moment of inertia (θ_i). The inertial torque (T_{ii}) generated by these components under acceleration correspond to the measured torque (T_{ti}) in the transducer. This value is considered a tare value for the evaluation of the net measured torque.

In the sequence of measurements and start-ups, Configuration II shows the inclusion of a reference mass moment of inertia (θ_r) to the main shaft. Now, the assembly's total inertia generates an inertial torque of ($T_{ii} + T_{ir}$), and that will correspond to a measured torque of (T_t). The net measured

Table 1. Correspondence between the parameters and assembly Configurations I and II of Figure 2

	Config. I	*Config. II*
MMI of the shaft	θ_i	$\theta_i + \theta_r$
Generated inertial torque	T_{ii}	$T_{ii} + T_{ir}$
Gross measured torque	T_{ti}	T_t
Net measured torque $(T_{ti} - T_t)$	T_{tl}	

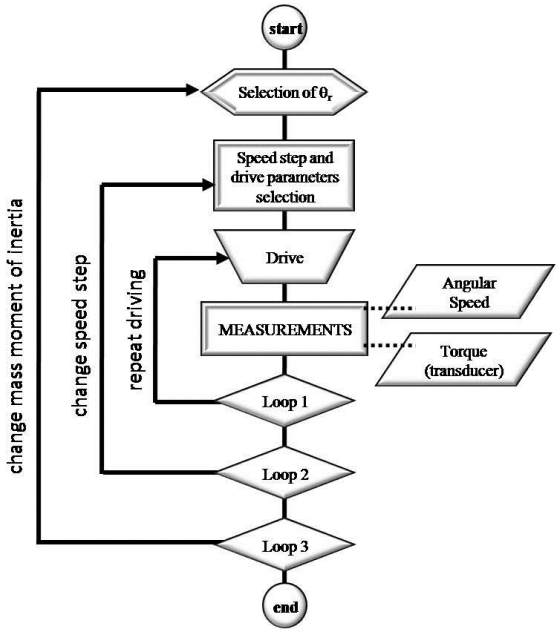

Figure 4. Sequence of operation to test different inputs to the sensor.

torque (T_{tl}) is the difference between the values measured in both configurations and corresponds to the evaluable inertial reference torque (T_{ir}). These correspondences between inertial configurations and torques can be found in Table 1.

Figure 4 shows the sequence of the operation of this system in terms of obtaining the sequential loadings, varying the conditions of inertia and accelerations that can be applied to a certain assembly of motor, shaft, and transducer. From this sequence, we can see that once an inertial condition is set, sequential speed steps and accelerations are applied to that configuration (loops 1 and 2). Thereafter, the inertial configuration is changed (loop 3), and the same sequence of acceleration and speeds must be applied. Therefore, the measured data of speed and torque are then evaluated to find the corresponding dynamic situations, and the net values can be calculated.

2.2. METHODS OF ANALYSIS

Two methods of analysis are proposed based on the relationship between the quantities involved. Both are applied from the same pack of measured data using only offline signal processing, including the calculation of the acceleration data from the differentiation of the speed data.

To help elucidate the proposed comparison methods, we use, to give the study a qualitative nature, a couple of real pieces of data, obtained from a set of experiments carried out during the research, together with an explanation and discussion of the method. The experimental assembly (Figure 5) was quite similar to that which was described in Figure 3, except for the fact that the encoder used for speed measurement was the slot type encoder included in the T12 torque transducer from HBM. The results of the driving of two inertial discs, named #D20 and #D40, under one acceleration profile are used here.

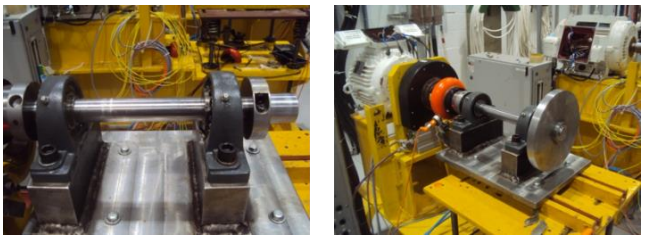

Figure 5. Experimental assembly for testing runs in the measuring shaft with the initial configuration (left) and with #D20 (right).

The first method is called 'direct calibration' and uses equation (2)(a), expanded in (2)(b), to evaluate the error results E, comparing the average values of reference torque T_{ir} to the measured net torque value at the transducer T_{tl}, both synchronized and indexed in time intervals as i.

$$E_{(i)} = \bar{T}_{tl(i)} - \bar{T}_{ir(i)} \tag{2.a}$$

$$E_{(i)} = \left(\bar{T}_{t(i)} - \bar{T}_{ti(i)}\right) - \left(\bar{\omega}_{(i)} \cdot \theta_r\right) \tag{2.b}$$

Figure 6 shows the T_{tl} and T_{ir} curves for each inertial configuration with discs, obtained from the averages of these parameters acquired in the runs inside the repetitions of 'loop 1' applied to the system and the corresponding results of E. Both inertial configurations were started with the same speed step and same acceleration profile, so they use the same averaged tare torque value.

From these graphical results, it is clear that there is a time dependency and tendency toward the error plots, even if they are different for the inertial configurations. The error for the loading side (up) of the curve is less than the error for the unloading side (bottom).

Due to the instability in the extremes of the pulse curves, where acceleration and inertial torque have almost zero values, what can be better noted in the acceleration curve of Figure 2 is that it would cause huge instability in the error analysis. This phenomenon induces the methodology to require a limitation for

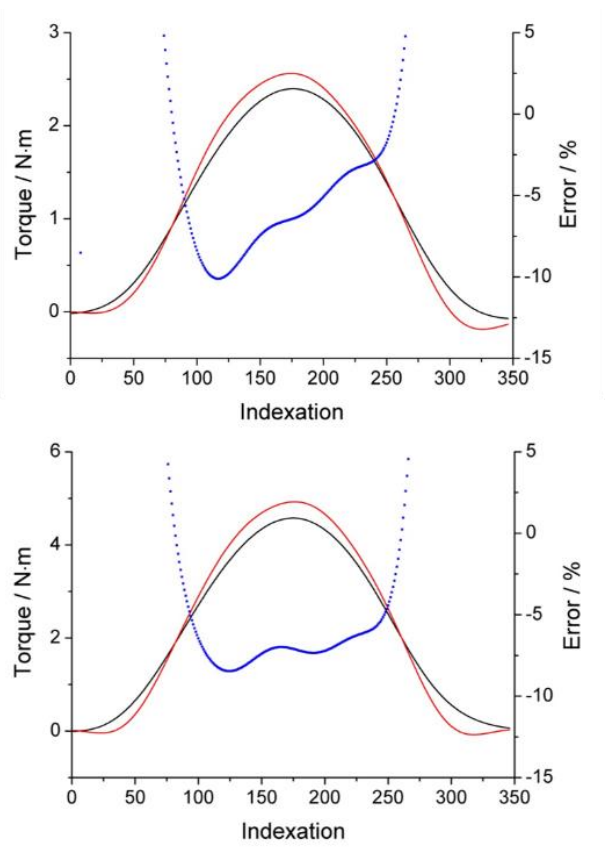

Figure 6. Error result (blue dot), between $\bar{T}_{tl(i)}$ (black line) and $\bar{T}_{ir(i)}$ (red line) according to the method of 'direct calibration' in the inertial configurations of (up) #D20 and (bottom) #D40.

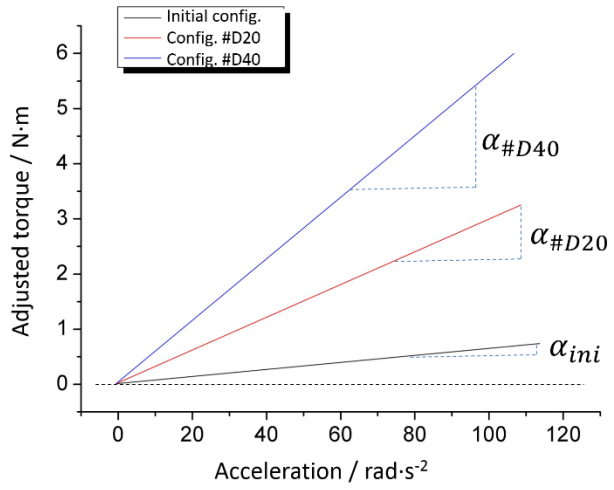

Figure 7. Graphical demonstration of the evaluable angular coefficients.

the studied range of torque within each comparison proceeding, corresponding to a pair of inertia and acceleration start-up parameters.

The second method is called 'indirect calibration' and tends to be a simpler process, with the analysis based on the linearity of the proposed principle and the differences between the angular slopes of linear fitting curves.

This method deals with the theoretical linear relationship between the reference acceleration and the torque value measured from the transducer. In order to keep the matter simple, data on T_t and $\dot{\omega}$ can be combined, and a linear fitting curve can be calculated, where there is now a new parameter known as 'adjusted torque' (T_{adj_t}), which is expressed in terms of $\dot{\omega}$ (equation (3)) and passes through the origin (0,0). This method does not demand the synchronization of torque readings.

$$T_{adj\_t} = \alpha \cdot \dot{\omega} \tag{3}$$

The coefficients (α) of these expressions are intended as comprising one for each inertial configuration under the same acceleration profile, including the initial configuration, also working here as a tare reference. Figure 7 shows a graphical interpretation of the method, calculating the angular coefficients

Table 2. Evaluated error E_θ for different inertial configurations.

Inertial config.	T_{cp} / N·m	θ_s /kg·m²	θ_r /kg·m²	E_θ
#D20	2.0	0.02355	0.02489	5.4 %
	1.5	0.02275		8.6 %
#D40	4.0	0.04650	0.04957	6.2 %
	3.5	0.04571		7.8 %

for the two inertial discs configurations, $\alpha_{\#D20}$ and $\alpha_{\#D40}$, of the shaft, calculated by means of the slope triangle method. The line with coefficient α_{ini} corresponds to the configuration without discs attached.

Once these coefficients are calculated, a net angular coefficient ($\theta_{\#Dxx}$) can be calculated for each inertial configuration, and that value can be compared to the MMI of reference ($\theta_{r\#Dxx}$), resulting in another error parameter ($E_{\theta xx}$), as shown in equation (4).

$$E_{\theta xx} = (\alpha_{\#Dxx} - \alpha_{ini}) - \theta_{r\#Dxx} = \theta_{\#Dxx} - \theta_{r\#Dxx} \tag{4}$$

Another interesting parameter that can be measured based on this method is the linearity deviation between the T_{adj_t} values (red line) and the measured T_t values (grey dots), as shown in Figure 8. This gives another idea of the behaviour of the sensor referring to the proposed physical principle.

From this graph, representing two runs for #D20, it is possible to observe that there is a better convergence (linearity deviation surrounding the zero value) on the upper part of the line, above 1.5 N·m, corresponding to the top of the pulse torque load curve. This refers to the necessity of determining a cut point in the torque domain (T_{cp}), restricting the analysis to a more stabilized region on the load regime.

In the same way as the direct calibration error, this phenomenon also influences the evaluation of error, and Table 2 shows the different values of relative E_θ for both inertial configurations with different torque cut points T_{cp}.

There, it can be noted that the closer the T_{cp} is from the top, the better error results it achieves, but the narrower is the range analysed.

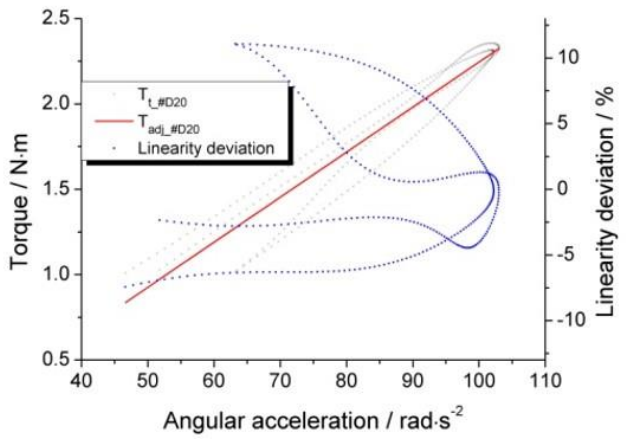

Figure 8. Linearity deviation for the configuration of #D20.

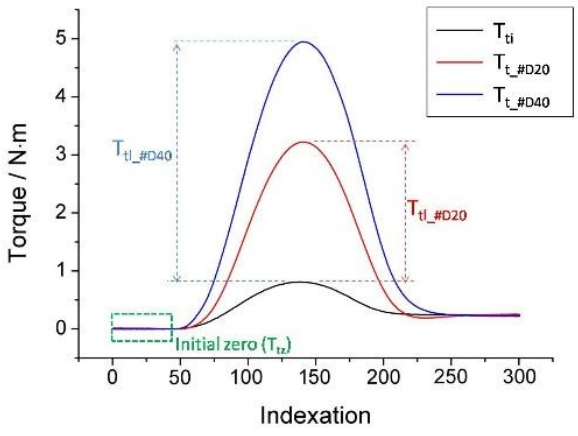

Figure 9. Synchronized (indexed intervals) torque curves.

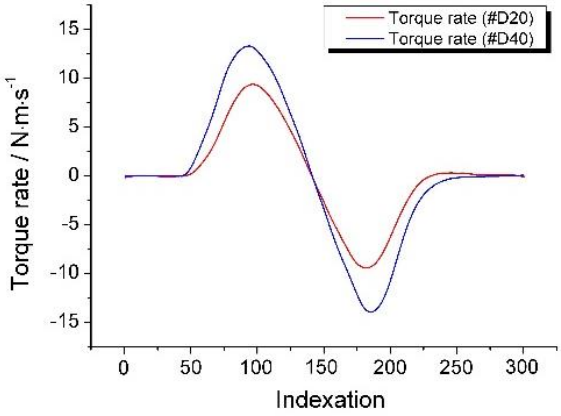

Figure 10. Torque rate curves for both inertial configurations.

By means of these experiments, the physical principle is validated. Figure 9 shows the torque curves T_t obtained from the averages for the measurements carried out during the loops with both inertial configurations and the same tare curve. The green box identifies the initial zero level, and there is an oscillation around this considered zero value, after the individual tare proceeding of each curve.

Figure 10 shows the achieved torque rates at these configurations, which were calculated as the first differentiation of the net torque curves. These maximum rates of torque achieved in the experiments were ±10 N·m·s^{-1} and ±15 N·m·s^{-1} for the #D20 and #D40 inertial configurations respectively.

3. HIGHLIGHTS CONCERNING UNCERTAINTY

The first approach to the evaluation of the uncertainty of measurement was presented in [2], with the identification of the basic components and their quantitative estimates. However, the development of the research demanded the increment and detailing of those components. Concerning the direct calibration method, for example, Figure 11 shows a good explanation of these developed components of uncertainty for the construction of U_E, mainly divided into uncertainty for the measured torque $U_{T_{tl}}$ and uncertainty of the reference inertial torque axis $U_{T_{ir}}$.

From that diagram, we can highlight that for the measured torque side, there are contributions from both inertial configurations I and II. Each configuration involves the

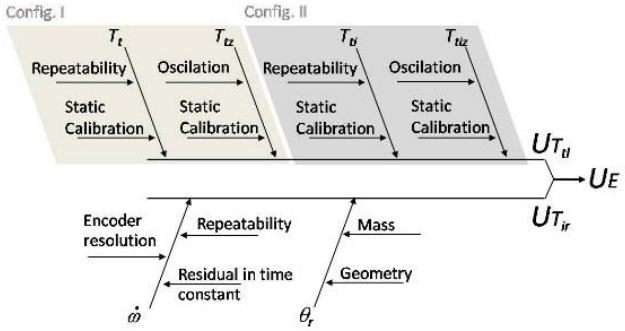

Figure 11. Main uncertainty contributions for U_E.

repeatability of the curves during loop 1 and after synchronization; the oscillation of initial zero levels (see Figure 9); and the static calibration uncertainty for the analysed point/range. This last contribution is important because there is a link between static and dynamic results.

For the inertial torque side, there are uncertainty contributions for the mass moment of inertia and acceleration. The MMI's contributions are related to the measurement of mass and geometry. The acceleration involves contributions from the constancy of the time intervals in the speed signal differentiation process, which is a parameter directly related to the acquisition system, from the encoder resolution and its static calibration (once there is no system for the calibration of speed), and from the repeatability of the acceleration curves during the loops.

An example of the behaviour of these uncertainty contributions can be seen in Figure 12. Three regions of the torque load curves are detached as the highest positive torque rate (left), the peak torque (middle), and the highest negative torque rate (right). The indexation references for these regions can be viewed in Figure 10.

It is possible, for instance, to evaluate the asymmetry between the components in relation to the central axis of the torque curve. The identification of the negative contribution of the component concerning the correlations between the uncertainties considered from the certificate of static calibration of the transducer is considered four times for each measured torque value, as identified as 'Static Calibration' in Figure 11. The uncertainty of the error (U_E) is expressed in units of torque and is presented as a confidence interval to be traced around the E curve, what can be seen as the red and blue lines.

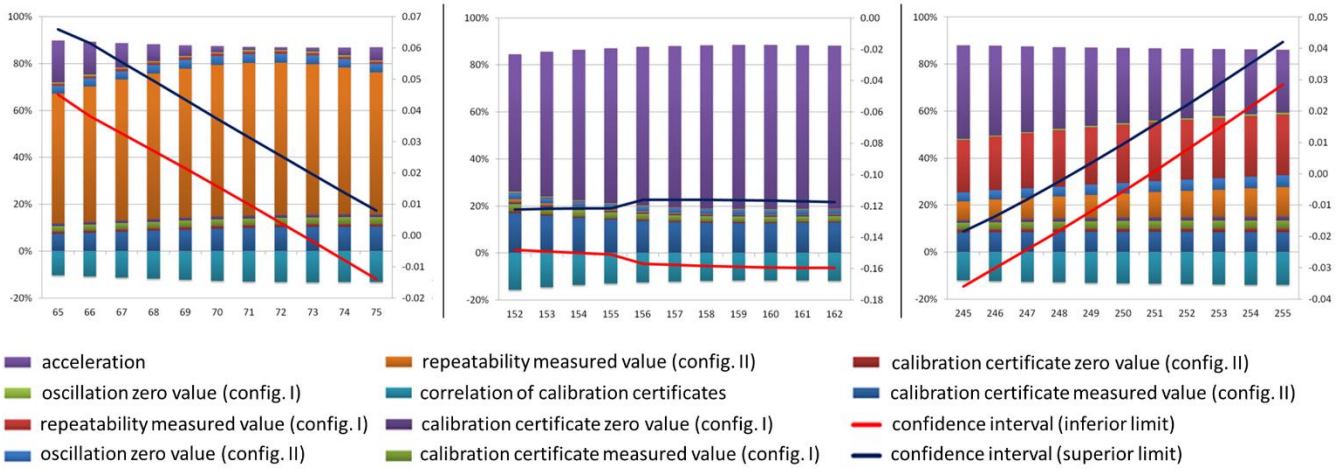

Figure 12. Composition of the uncertainty budget considering each contribution parameter of uncertainty in the three regions of the torque load curve: highest positive torque rate (left), peak torque, torque rate null (middle), and the highest negative torque rate (right).
Axis: Indexation (X), Partial relative contribution (left Y) and Error in N·m (right Y).

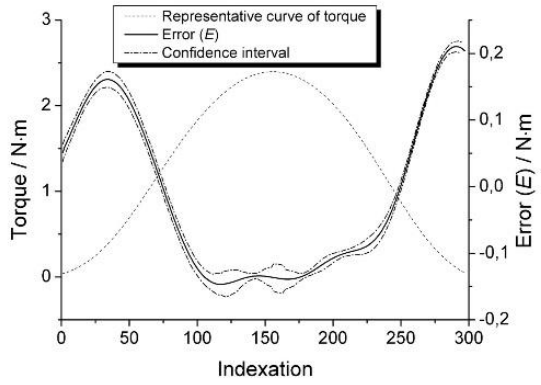

Figure 13. Torque load curve with the Error and the respective uncertainty interval envelope.

For the indirect calibration method, the main contributions of uncertainty will be about the method for calculating the linear fitting curve.

3.1. HOW TO REPORT THE RESULTS

The dynamic calibration proposal included two different methods of analysis, what can be interesting to be joint in a same test report. Nevertheless, the report should contain all the parameters of interest, due to the vast possibility of combinations, such as the following suggestions:

- Characterize the torque pulses of interest (peak torque, maximum torque rate, acceleration or deceleration, clockwise or anticlockwise);
- Highlight the static uncertainties;
- Report kinematic conditions: speed step, acceleration times, and reference MMIs used;
- Report E and its uncertainty U_E in the graphic mode or select the most interesting points in the load curve and report those parameters for each torque point in a table. Figure 13 shows the torque load curve for the experiment with the #D20 inertia configuration as an example. In the graph, there is the average $\bar{T}_{tl}$ and the confidence interval for the uncertainty U_E.
- Report E_θ together with the corresponding T_{cp}, such as in Table 2.

4. CONCLUSION AND OUTLOOK

This paper has focused on the need to better evaluate, in the time domain, those regimes of torque with high variations of quantity. Two calibration evaluation methods are presented.

The results obtained from the direct calibration method showed the temporal dependency of errors, and the indirect method can evaluate hysteresis and linearity deviations from the physical principle adopted for the realization of the reference dynamic torque. Pieces with known moments of inertia and accelerations profiles are combined to give different torque load profiles.

The two evaluation methods are complementary, originate from the same measurement data, and can join the same 'calibration report'.

Uncertainty of measurement must be part of a parallel discussion. The presented uncertainty results could be considered to evidence the interesting behaviour of the different contributions on the different periods of the torque load curve and the time domain.

The capacity of a system to reach high torque rates depends on the capacity of the electric motor to accelerate the shaft within its limits of maximum acceleration torque. From now on, it is necessary to repeat the experiments under different conditions, revalidating the method and analysing the proposed assembly.

REFERENCES

[1] DIN 51309: Materials testing machines - Calibration of static torque measuring devices (German standard), DIN (2005).

[2] C. Bartoli et al, Dynamic calibration of force, torque and pressure sensors, Proc. of the 22nd IMEKO TC3 Conference, Cape Town, Republic of South Africa, 3 – 5 February 2014, https://www.imeko.org/publications/tc22-2014/IMEKO-TC3-TC22-2014-007.pdf

[3] J. Schleichert, I. Rahneberg, R. R. Marangoni, T. Fröhlich, Calibration and uncertainty analysis for multicomponent force/torque measurements, Technisches Messen (2016), DOI: https://doi.org/10.1515/teme-2016-0048

[4] J. Schleichert, I. Rahneberg, T. Fröhlich, Calibration of a novel six-degree-of-freedom force/torque measurement system, Int. J. Mod. Phys. Conf. Ser. 24 (2013), pp. 1360017-1 - 9 DOI: https://doi.org/10.1142/S2010194513600173

[5] R. S. Oliveira, H. A. Lepikson, T. Fröhlich, R. Theska, R. R. Machado, 'Dynamic Calibration of Torque Transducers Applying Angular Acceleration Pulses', Proc. of the 23rd IMEKO TC3 Conference, Helsinki, Finland, 30 May – 1 June 2017, https://www.imeko.org/publications/tc3-2017/IMEKO-TC3-2017-025.pdf

[6] R. S. Oliveira, H. A. Lepikson, T. Fröhlich, R. Theska, W. A. Duboc, 'A New Proposal for the Dynamic Test of Torque Transducers', Proc. of the XXI IMEKO World Congress, Prague, Czech Republic, 30 August – 4 September 2015, https://www.imeko.org/publications/wc-2015/IMEKO-WC-2015-TC3-041.pdf

[7] R. S. Oliveira, H. A. Lepikson, T. Fröhlich, R. Theska, Simon Winter, A new approach to test torque transducers under dynamic reference regimes, Measurement 58 (2014), pp. 354-362, DOI: https://doi.org/10.1016/j.measurement.2014.09.020

[8] R. S. Oliveira et al., Estimate of the inertial torque in rotating shafts - a metrological approach to signal processing, Journal of Physics: Conference Series 648 (2015) 012019, 11 p. DOI: https://doi.org/10.1088/1742-6596/648/1/012019

[9] G. Wegener, T. Bruns, Traceability of torque transducers under rotating and dynamic operating conditions, Measurement 42 (2009) 10, pp. 1448-1453, DOI: https://doi.org/10.1016/j.measurement.2009.08.007

[10] L. Klaus, T. Bruns, M. Kobusch, Determination of Model Parameters for A Dynamic Torque Calibration Device, Proc. of the XX IMEKO World Congress, Busan, Republic of Korea, 9 – 14 September 2012, https://www.imeko.org/publications/wc-2012/IMEKO-WC-2012-TC3-O33.pdf

[11] A. Brüge, Fast Torque Calibrations Using Continuous Procedures, Proc. of the 20th IMEKO TC3 conference, Celle, Germany, 24 – 26 September 2002, https://www.imeko.org/publications/tc3-2002/IMEKO-TC3-2002-016.pdf

[12] A.Brüge, R. Konya, Investigation on transducers for transfer or reference in continuous torque calibration, Proc. of the 19th IMEKO TC3 Conference, Cairo, Egypt, 19 – 23 February 2005, https://www.imeko.org/publications/tc3-2005/IMEKO-TC3-2005-035u.pdf

[13] S. Nattapon, S. Tassanai, A Comparison of Purely Static and Continuous Torque Calibration Procedure, Proc. of the 22nd IMEKO TC3 Conference, Cape Town, Republic of South Africa, 3 – 5 February, 2014, https://www.imeko.org/publications/tc3-2014/IMEKO-TC3-2014-011.pdf